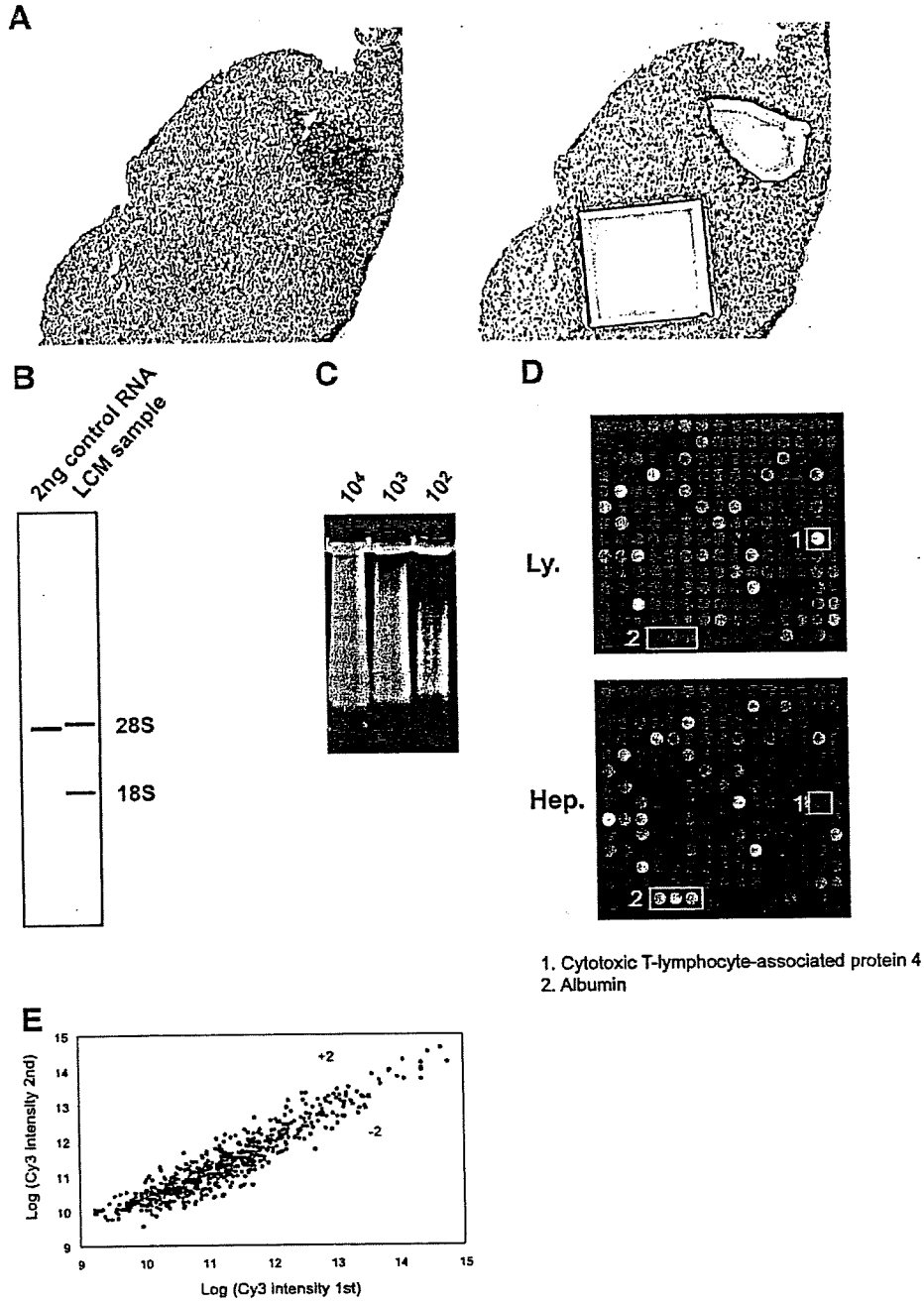

Fig. 1. Optimization of LCM and cDNA microarray analysis. (A) Toluidine blue staining of liver biopsy specimens before (left) and after (right) LCM. (B) Electrophoresis of isolated RNA using an Agilent 2001 bioanalyzer. (C) Two round-amplified aRNA from 10^2-10^4 excised hepatocytes. (D) Typical hybridization result from LCM samples. (E) Correlation of signal intensity between first and second amplified genes. Two values were significantly correlated ($P < .001$, $r^2 = .97$) within 2-fold differences.

rayTools (http://linus.nci.nih.gov/BRB-ArrayTools.htm). The filtered data were log-transferred, normalized, centered, and applied to the average linkage clustering with centered correlation. A class prediction was performed by compound covariate predictor incorporating genes that were differentially expressed at the $P = .002$ significance

Table 2. Supervised Learning Methods to Differentiate CHB and CHC

Classifier Category	Clinical Groups	Total Number of Cases	Number of Cases Misclassified	Classifier *P* Values	Number of Genes in the Classifiers ($P < .002$)
HBV versus HCV	HBV	19	1	<0.001	160
	HCV	18	3		
Histological stage	F1F2	17	10	0.402	55
	F3F4	20	7		
Histological activity	A0A1	13	6	0.173	106
	A2A3	24	6		
Age	≥50	22	9	0.298	39
	<50	15	6		
ALT at biopsy	≥80	14	7	0.200	21
	<80	23	6		

level as assessed by the random variance *t* test (BRB-ArrayTools). The univariate *t* test values for comparing the classes were used as the weights. The cross-validated misclassification rate was computed and at least 2,000 permutations were performed for a valid permutation *P* value. The Fisher and Kolmogorov-Smirnov tests were performed for gene ontology (GO) comparison ($P < .005$) (BRB-ArrayTools).

Pathway Analysis of Expression Data. The pathway analysis of the differentially expressed genes was performed using MetaCore software suite (GeneGo, St. Joseph, MI). Possible networks were created according to the list of the differentially expressed genes using the MetaCore database, a unique, curated database of human protein-protein and protein-DNA interactions; transcription factors; and signaling, metabolic, and bioactive molecules. The *P* value was calculated as:

$$p\text{-Value} = \frac{R!n!(N-R)!(N-n)!}{N!} \sum_{i=\max(r,R+n-N)}^{\min(n,R)} \frac{1}{i!(R-i)!(n-i)!(N-R-n+i)!}$$

where N is total number of nodes in the MetaCore database, R the number of network objects corresponding to the genes list, n the total number of nodes in each small network generated from the genes list, and r the number of nodes with data in each small network generated from the genes list. Moreover, direct interactions among the differentially expressed genes were examined. Each connection represents a direct, experimentally confirmed, physical interaction.

SAGE. Total RNA isolated from each of 3 patients with CH-B or CH-C was mixed to 200 μg in total, and polyadenylated RNA was extracted using a FastTrac mRNA Purification Kit (Invitrogen). The SAGE protocol was as described.[20,21] SAGE libraries were sequenced at random using an ABI Prism 377 DNA Sequencer and BigDye Terminator Cycle Sequencing Kit (PE Applied Biosystems, Foster City, CA). Sequenced files were analyzed with the SAGE version 1.00 software.

Quantitative Real-time Detection PCR. We performed quantitative real-time detection PCR (RTD-PCR) using TaqMan Universal Master Mix (PE Applied Biosystems). Primer pairs and probes for MxA, IP10, IFI15, OAS2, GZMA, TP53, PDECGF, IFNG, DIABLO, FGFB, BGA2, CASP9, PEX5, ANGPT1, VEGF, and β-actin were obtained from TaqMan assay reagents library. Results were expressed as means ± SEM. Significance was tested by 1-way ANOVA with Bonferroni's methods and differences were considered statistically significant at $P < .05$.

Results

Optimization of LCM and cDNA Microarray Analysis. Before analysis of region-specific gene expression, the sensitivity and reliability of linear aRNA amplification was examined. The quality and degradation of the isolated RNA were estimated after electrophoresis using an Agilent 2001 bioanalyzer (Fig. 1B). We successfully amplified aRNA from 10^2-10^4 excised hepatocytes with 2 rounds of amplification (Fig. 1C). The estimated amount of isolated RNA from around 150 excised hepatocytes (Fig. 1A) was 5-10 ng, and 10-20 μg of aRNA was obtained by 2 rounds of amplification, assuming that a 25×10^4-fold amplification (500-fold by single amplification) was carried out. A typical hybridization result is shown in Fig. 1D. Cytotoxic T lymphocyte-associated protein 4

Fig. 2. (A) Hierarchical clustering analysis of gene expression in hepatocytes and liver-infiltrating lymphocytes. Hep, hepatocyte; Ly, lymphocyte; B, hepatitis B; C, hepatitis C. (B) Hierarchical clustering analysis of 1,360 filtered genes (we excluded genes with an expression level within 1.5-fold of median value in more than 80% of samples) demonstrated more clear clusters of CH-B and CH-C.

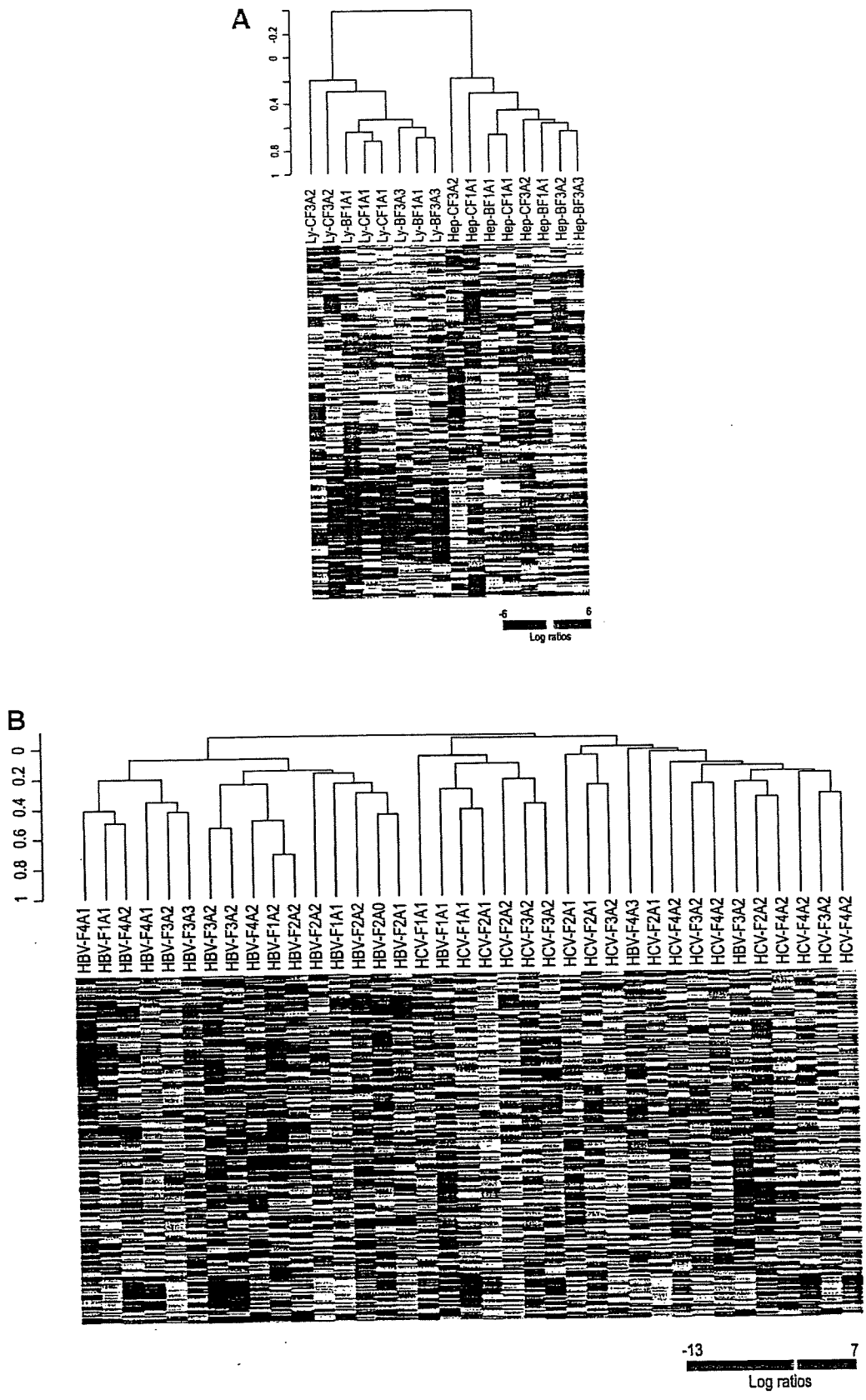
A
1 0.8 0.4 0 -0.2
Ly-CF3A2
Ly-CF3A2
Ly-BF1A1
Ly-CF1A1
Ly-CF1A1
Ly-BF3A3
Ly-BF1A1
Ly-BF3A3
Hep-CF3A2
Hep-CF1A1
Hep-BF1A1
Hep-CF1A1
Hep-CF3A2
Hep-BF1A1
Hep-BF3A2
Hep-BF3A3
-6
6
Log ratios
B
1 0.8 0.6 0.4 0.2 0
HBV-F4A1
HBV-F1A1
HBV-F4A2
HBV-F4A1
HBV-F3A2
HBV-F3A3
HBV-F3A2
HBV-F3A2
HBV-F4A2
HBV-F1A2
HBV-F2A2
HBV-F2A2
HBV-F1A1
HBV-F2A2
HBV-F2A0
HBV-F2A1
HCV-F1A1
HBV-F1A1
HCV-F1A1
HCV-F2A1
HCV-F2A2
HCV-F3A2
HCV-F3A2
HCV-F2A1
HCV-F2A1
HCV-F3A2
HBV-F4A3
HCV-F2A1
HCV-F4A2
HCV-F3A2
HCV-F4A2
HBV-F3A2
HCV-F2A2
HCV-F4A2
HCV-F4A2
HCV-F3A2
HCV-F4A2
-13
7
Log ratios

Fig. 2

was predominantly expressed in liver-infiltrating lymphocytes, whereas albumin was predominantly expressed in hepatocytes (Fig. 1D). To determine whether multiple amplifications affected the original gene expression, the signal intensities of first- and second-round amplified genes were compared. There was a significant correlation between the 2 values ($P < .001$, $r^2 = .97$), within a 2-fold difference (Fig. 1E), suggesting that the linear amplification procedure maintained the original level of gene expression.

Identification of Genes Differentially Expressed in Hepatocytes and Liver-Infiltrating Lymphocytes. Pairwise *t* test comparisons were applied and differentially expressed genes were identified in lymphocytes and hepatocytes in 4 patients with CH-B and 4 patients with CH-C (Supplementary Table 1-1). In hepatocytes, liver-specific proteins and enzymes such as fibrinogen, afamin, and cytochrome P450 were all expressed. In lymphocytes, cytokines, chemokines, and lymphocyte surface markers such as interleukin-7 receptor, chemokine (C-X-C motif) receptor 4, CD83 antigen, and CD69 antigen were all expressed (Supplementary Table 1-2). Hierarchical clustering analysis of gene expression in hepatocytes and liver-infiltrating lymphocytes demonstrated clear differences in gene expression (Fig. 2). Representative differentially expressed genes in lymphocytes and hepatocytes in CH-B and CH-C are summarized in Supplementary Tables 2-1, 2-2, 3-1, and 3-2.

Supervised and Nonsupervised Learning Methods to Classify Gene Expression Profiling According to Different Clinical Parameters. To examine which clinical parameters contributed to the changes in gene expression, supervised and nonsupervised learning methods were applied to classify gene expression profiles. The gene expression profiles of whole liver biopsy specimens, obtained from 19 patients with CH-B and 18 with CH-C, were analyzed. Hierarchical clustering analysis; a nonsupervised learning method, using 9641 nonfiltered genes, clearly demonstrated 2 clusters in CH-B and CH-C with a few exceptions (data not shown). Hierarchical clustering analysis with 1360 filtered genes (we excluded genes with an expression level within 1.5-fold of the median value in more than 80% of samples) demonstrated clearer clusters in CH-B and CH-C (Fig. 2B). Supervised learning methods based on the compound covariate predictor revealed that, among various clinical parameters including etiology (HBV or HCV), histological stage (F_1F_2 or F_3F_4), activity (A_0A_1 or A_2A_3), age (≥50 or <50 years), and alanine aminotransferase (ALT) level at biopsy (≥80 or <80 IU/mL), only etiology significantly classified these patients (Table 2). Thus, HBV or HCV infection determines gene expression to a greater degree than any other clinical parameters, such as histological stage and disease activity.

Differentially Expressed Genes in CH-B and CH-C Hepatic Lesions. The 160 genes were differentially expressed in CH-B and CH-C by class prediction analysis ($P < .005$); representative genes (greater than 3-fold difference in *t* value) are listed in Tables 3 and 4. Based on the expression profiles of hepatocytes and lymphocytes isolated using LCM, genes expressed in both hepatocytes and lymphocytes are described as Hep/Ly (Tables 3 and 4). Genes expressed at a significantly greater level in hepatocytes than lymphocytes were described as Hep. Genes expressed at a significantly greater level in lymphocytes than hepatocytes were described as Ly. In CH-B, genes involved in cell cycle arrest and induction of apoptosis were preferentially expressed. Several hepatocyte-specific and apoptosis-inducing genes such as Diablo homolog (cytochrome c/apaf-1/caspase-9 pathway activator) and BCL2-associated athanogene 2 (inhibitor of heat shock protein 70) were upregulated (Table 3, Fig. 7). In CH-C, cell cycle accelerating, immune-related, and antigen-presenting genes were preferentially upregulated. Many type 1 IFN-induced genes such as IFN-α-inducible protein 27 and IFN-α-inducible protein (clone IFI-15K) were upregulated in CH-C. The induction of these genes was confirmed by examining gene expression in Huh-7 cells treated with recombinant IFN-α (Tables 3 and 4, Fig. 7).

The frequent pathway processes observed in CH-B and CH-C using MetaCore are shown in Table 5. Induction of genes related to apoptosis (caspase activation via cytochrome C), transcription, and fibrosis (intermediate filament-based process and TGF-β receptor signaling pathway) were upregulated in CH-B, whereas genes related to immune reaction (defense response, antigen presentation, Golgi vesicle transport, and ubiquitin cycle), lipid metabolism (regulation of cholesterol absorption), and epidermal growth factor receptor (EGFR) signaling were upregulated in CH-C. This suggests that there are different signaling pathways in CH-B and CH-C.

Go Comparison of Expressed Genes in CH-B and CH-C Hepatic Lesions. The analysis of differentially expressed genes could underestimate the presence of mean full signaling pathways that were coordinately upregulated or downregulated, with subtle differences at an individual gene level. The biological significance of these coordinately regulated signaling pathways has recently been demonstrated.[22] Therefore, we applied the GO comparison tool to expressed genes in CH-B and CH-C hepatic lesions. The comparison tool provided a list of GO categories that were coordinately regulated between CH-B and CH-C.

Table 3. Differentially Upregulated Genes in Liver of Chronic Hepatitis B

Gene	GenBank ID	P Value	t Value HBV/HCV*	Hep/Ly	GO: Molecular Function
Viral genome					
HBV-core	X01587	0.000	6.69	Hep	Viral genome
Cell cycle and growth related					
V-ets erythroblastosis virus E26 oncogene homolog 2	NM_005239	0.001	3.97	Hep/Ly	skeletal development
RAP2A, member of RAS oncogene family	AI698376	0.000	3.91	Hep/Ly	signal transduction
Melanoma antigen, family C, 1	NM_005462	0.001	3.76	Hep/Ly	regulation of transcription
Cell division cycle 27	NM_001256	0.001	3.54	Hep/Ly	cell proliferation
Cyclin H	NM_001239	0.000	3.10	Hep/Ly	DNA repair
Immune response					
Interferon regulatory factor 6	NM_006147	0.000	3.80	Hep	regulation of transcription, DNA-dependent
Proteoglycan 2, bone marrow	R28336	0.001	3.65	Hep/Ly	defense response to bacteria
Chemokine (C-C motif) ligand 16	AW827147	0.001	3.49	Hep/Ly	chemokine activity
Janus kinase 2 (a protein tyrosine kinase)	NM_004972	0.001	3.48	Ly	JAK-STAT cascade
Chemokine (C-X-C motif) receptor 3	NM_001504	0.000	3.03	Hep/Ly	G-protein coupled receptor protein signaling pathway
Cell death					
BCL2-associated athanogene 2	NM_004282	0.000	3.95	Hep	apoptosis
Fas (TNFRSF6) associated factor 1	AA831837	0.001	3.74	Hep/Ly	apoptosis
Proline dehydrogenase (oxidase) 1	R88591	0.000	3.73	Hep/Ly	induction of apoptosis by oxidative stress
Caspase 9, apoptosis-related cysteine protease	NM_032996	0.001	3.58	Hep/Ly	apoptotic program
Purinergic receptor P2X, ligand-gated ion channel, 1	NM_002558	0.003	3.52	Hep/Ly	apoptosis
Tumor suppressing subtransferable candidate 1	NM_003310	0.002	3.35	Hep/Ly	apoptosis
Tumor necrosis factor (ligand) superfamily, member 11	NM_033012	0.002	3.25	Hep	cell differentiation
Diablo homolog (*Drosophila*)	NM_019887	0.004	3.04	Hep	apoptosis
Cell communication					
Nexilin (F actin binding protein)	NM_144573	0.000	4.15	Hep/Ly	unknown
Neurogranin (protein kinase C substrate, RC3)	NM_006176	0.000	4.09	Hep	signal transduction
Collagen, type XV, alpha 1	NM_001855	0.000	4.08	Hep/Ly	extracellular matrix
Chromogranin B (secretogranin 1)	NM_001819	0.001	3.47	Hep/Ly	hormone activity
Prostaglandin I2 (prostacyclin) receptor (IP)	NM_000960	0.001	3.42	Ly	G-protein signaling
Integral membrane protein 2C	NM_030926	0.002	3.36	Ly	integral to membrane
Sperm autoantigenic protein 17	NM_017425	0.002	3.26	Hep/Ly	cAMP-dependent protein kinase regulator activity
Talin 2	AF007154		3.18	Ly	cell adhesion
Cadherin 16, KSP-cadherin	AI241319	0.003	3.11	Hep	cell adhesion
Syntaxin binding protein 6 (amisyn)	AA281449	0.004	3.03	Ly	cell adhesion
Stress response					
RAD51-like 1 (*S. cerevisiae*)	NM_002877	0.000	3.78	Hep/Ly	DNA repair
Metallothionein 1X†	BC053882	0.001	3.44	Hep	electron transport
Siah-interacting protein	AA069322	0.002	3.08	Hep/Ly	ubiquitin cycle
Metallothionein 2A‡	NM_005953	0.004	3.03	Hep	copper ion homeostasis
F-box and leucine-rich repeat protein 2	NM_012157	0.000	3.01	Hep/Ly	ubiquitin cycle
Development					
Wolf-Hirschhorn syndrome candidate 1	NM_133335	0.001	4.51	Hep/Ly	morphogenesis
Homeo box B2	AI292043	0.001	3.87	Hep/Ly	development
Neurogenic differentiation 1	NM_002500	0.000	3.38	Hep/Ly	cell differentiation
Opiate receptor-like 1	NM_000913	0.004	3.29	Hep/Ly	G-protein coupled receptor protein signaling pathway
Wingless-type MMTV integration site family, member 2B	NM_024494	0.002	3.14	Hep/Ly	frizzled-2 signaling pathway
Cell motility					
Oligophrenin 1	R81942	0.001	3.80	Hep/Ly	rho GTPase activator activity
ATP-binding cassette, subfamily C, member 9	H16193	0.004	3.06	Hep	transporters
Transporter					
Sodium channel, voltage gated, type VIII, alpha	NM_014191	0.004	3.78	Hep/Ly	cation transport
Enzymes					
HMT1 hnRNP methyltransferase-like 6 (*S. cerevisiae*)	NM_018137	0.001	4.44	Hep/Ly	s-adenosylmethionine-dependent methyltransferase
Chymotrypsin-like	NM_001907	0.001	3.74	Hep/Ly	negative regulation of blood coagula
Aspartoacylase (aminocyclase) 3§	NM_080658	0.005	3.26	Hep/Ly	metabolism
Transcription and signal transduction					
Hepatocyte nuclear factor 4, gamma	AW273065	0.000	4.38	Hep/Ly	regulation of transcription
Nuclear receptor coactivator 6	NM_014071	0.000	3.98	Hep/Ly	DNA recombination
Protein kinase C, gamma	NM_002739	0.001	3.88	Hep/Ly	intracellular signaling cascade
T-box 2	NM_005994	0.000	3.82	Hep/Ly	development
Zinc finger protein 167	NM_018651	0.003	3.49	Hep/Ly	regulation of transcription, DNA-dependent
Small nuclear ribonucleoprotein polypeptide A	AI491862	0.002	3.37	Hep/Ly	intracellular signaling cascade
Zinc finger protein 266	NM_198058	0.002	3.03	Ly	regulation of transcription, DNA-dependent

*The univariate *t*-statistics for comparing the classes are used as the weights. †3.9-fold induction, ‡7.7-fold induction, and §1.8-fold induction by IFN-α in Huh-7 cells

In accordance with pathway analysis, antigen-presenting major histocompatibility complex molecules and IFN-α-induced genes were preferentially upregulated in CH-C (Table 6, Fig. 3). Genes related to apoptosis, DNA repair and cell death were upregulated in CH-B. DNA repair and apoptosis-related transcription factors were upregulated in CH-B, whereas anti-apoptosis and cell proliferation-related transcription factors were upregulated in CH-C. Platelet activating factor was upregulated in CH-C. As for metabolism-related gene regulation, peroxisome-associated genes were

Table 4. Differentially Upregulated Genes in Liver of Chronic Hepatitis C

Gene	GenBank ID	P Value	t Value HCV/HBV	Hep/Ly	IFN induced	GO: biological process
Cell cycle and growth related						
Hect domain and RLD 5	NM_016323	0.000	4.50	Hep/Ly	7.7	regulation of cyclin dependent protein kinase activity
Inhibitor of growth family, member 4	NM_198287	0.001	3.50	Hep/Ly		grow arest
Phosphoinositide-3-kinase, class 3	AI446184	0.001	3.42	Hep/Ly		inositol or phosphatidylinositol kinase activity
Non-metastatic cells 1, protein (NM23A) expressed in	NM_000269	0.002	3.28	Hep		CTP biosynthesis
Mitogen-activated protein kinase kinase kinase 10	AI991621	0.003	3.23	Hep/Ly		JNK cascade
Immune responces						
Interferon, alpha-inducible protein 27	NM_005532	0.000	6.29	Hep	2.4	response to pest, pathogen or paras
Interferon, alpha-inducible protein (clone IFI-15K)	NM_005101	0.000	4.65	Hep/Ly	27.9	cell-cell signaling
Myxovirus (influenza virus) resistance 1	NM_002462	0.000	4.28	Hep/Ly	49.9	
Cold autoinflammatory syndrome 1	NM_183395	0.000	4.14	Ly		inflammatory response
Interferon-stimulated transcription factor 3, gamma 48kD	NM_006084	0.000	3.89	Hep/Ly	1.8	immune response
Beta-2-microglobulin	NM_004048	0.001	3.63	Hep/Ly	2.7	antigen presentation, endogenous antigen
2'-5'-oligoadenylate synthetase 2 (69-71 kD)	AA731148	0.001	3.49	Hep/Ly	3.3	immune response
Interferon-induced protein 44-like	NM_006820	0.001	3.42	Ly	4.5	immune response
Apolipoprotein L, 3	AW002766	0.003	3.23	Ly		inflammatory response
Immunoglobulin kappa constant	BC062732	0.004	3.04	Ly		immune response
Cell death						
Defender against cell death 1	NM_001344	0.000	4.11	Hep/Ly		apoptosis
HIV-1 Tat interactive protein 2, 30kDa	NM_006410	0.004	3.03	Hep/Ly		induction of apoptosis
Cell communication						
Major histocompatibility complex, class I, C	NM_002117	0.001	3.74	Hep/Ly		antigen presentation
CD97 antigen	NM_078481	0.001	3.72	Ly		cell adhesion
Major histocompatibility complex, class I, B	NM_005514	0.002	3.38	Hep/Ly	1.9	antigen presentation
Carcinoembryonic antigen-related cell adhesion molecule 5	NM_004363	0.002	3.30	Hep/Ly		integral to plasma membrane
Major histocompatibility complex, class II, DQ beta 1	NM_002123	0.002	3.25	Ly		antigen presentation
Major histocompatibility complex, class II, DR beta 4	NM_022555	0.002	3.25	Hep/Ly		antigen presentation
Dystroglycan 1 (dystrophin-associated glycoprotein 1)	AI684076	0.003	3.14	Hep/Ly		extracellular matrix
Dipeptidylpeptidase 6	NM_130797	0.004	3.11	Hep/Ly		integral to membrane
Ubiquitin and proteasome system						
Proteasome (prosome, macropain) subunit, beta type, 8	U17496	0.000	4.55	Hep/Ly		immune response
Ubiquitin D	NM_006398	0.003	3.13	Ly	2.1	antimicrobial humoral response
Proteasome (prosome, macropain) 26S subunit, non-ATPase, 2	NM_002808	0.004	3.05	Hep/Ly		regulation of cell cycle
Translation						
Eukaryotic translation elongation factor 1 beta 2	AI262506	0.000	4.46	Ly		protein biosynthesis
Eukaryotic translation initiation factor 1A, Y-linked	NM_004681	0.003	3.19	Hep/Ly	5.3	protein biosynthesis
Lipid metabolism						
Diacylglycerol O-acyltransferase homolog 1 (mouse)	NM_012079	0.002	3.31	Hep/Ly		O-acyltransferase activity
24-dehydrocholesterol reductase	NM_014762	0.003	3.19	Hep		cholesterol biosynthesis
Carnitine palmitoyltransferase II	NM_000098	0.005	3.01	Hep/Ly		fatty acid beta-oxidation
Nucleotide metabolism						
Adenosine deaminase, RNA-specific	NM_015841	0.001	3.46	Hep/Ly		RNA editing
Topoisomerase (DNA) I	J03250	0.003	3.22	Hep/Ly		DNA unwinding
THO complex 1	L36529	0.003	3.15	Hep/Ly		nuclear mRNA splicing, via spliceosome
Karyopherin alpha 3 (importin alpha 4)	NM_002267	0.003	3.14	Hep/Ly		NLS-bearing substrate-nucleus import
Nicotinamide nucleotide adenylyltransferase 1	NM_022787	0.004	3.06	Hep/Ly		NAD biosynthesis
Nuclear autoantigenic sperm protein (histone-binding)	M97856	0.005	3.00	Hep/Ly		DNA packaging
Ribonucleotide reductase M2 polypeptide	NM_001034	0.005	3.00	Ly		DNA replication
G protein binding protein						
Regulator of G-protein signalling 10	NM_002925	0.002	3.38	Hep/Ly		signal transduction
Transcription and signal transduction						
Staphylococcal nuclease domain containing 1	NM_014390	0.000	4.60	Hep/Ly		development
Ring-box 1	NM_014248	0.001	3.61	Ly		protein ubiquitination
Trophinin	NM_177558	0.001	3.44	Ly		embryo implantation
Forkhead box F1	AI453333	0.001	3.18	Hep/Ly	2.5	regulation of transcription, DNA-dependent
Nuclear antigen Sp100	M60618	0.003	3.02	Hep/Ly	5.8	regulation of transcription, DNA-dependent
Zinc finger protein 211	NM_198855	0.004	3.02	Ly		regulation of transcription, DNA-dependent
GA binding protein transcription factor, beta subunit 2, 47kDa	NM_181427	0.004	3.02	Hep/Ly		regulation of transcription, DNA-dependent
LIM protein (similar to rat protein kinase C-binding enigma)	AI445592	0.004	3.01	Hep/Ly		heart development
Hematopoietic cell-specific Lyn substrate 1	NM_005335	0.005	3.00	Ly		intracellular signaling cascade
ADP-ribosylation factor 5	M57567	0.005	3.00	Hep/Ly		intracellular protein transport

upregulated in CH-B, whereas cholesterol biosynthesis was upregulated in CH-C.

To investigate these findings in more detail, lymphocytes and hepatocytes were separately isolated by LCM and their gene expression was examined (Table 6, Fig. 4A, Fig. 7). Cyclophilin A and cyclophilin C, encoding peptidyl-prolyl cis-trans isomerases, were upregulated in CH-C. A recent report describes inhibition of HCV replication in Huh-7 cells by cyclophilin.[23,24] The upregulation of ssDNA-binding genes, such as p53 and RAD, and the relative downregulation of mitochondrial genes in hepatocytes, in CH-B, reflect a strong DNA damage response inducing apoptosis. Many IFN-α-induced genes were upregulated in hepatocytes rather than lymphocytes in CH-C.

CD4, CD8, linker for activation of T cells, and pro-apoptotic genes were upregulated in lymphocytes

Table 5. Pathway Analysis

Frequent Pathway Process	P Value
Whole liver tissue in CHB (n = 19)	
Caspase activation via cytochrome c	7.04E-11
Regulation of transcription, DNA-dependent	1.66E-12
Intermediate filament-based process	1.24E-07
Calcium ion transport	9.08E-08
Regulation of blood pressure	2.94E-07
Protein amino acid phosphorylation	4.04E-07
Regulation of angiogenesis	5.35E-09
TGF-beta receptor signaling pathway	8.08E-11
Whole liver tissue in CHC (n = 20)	
Defense response	3.27E-06
Antigen presentation, endogenous antigen	6.79E-06
Golgi vesicle transport	5.22E-07
Lipid catabolism	6.61E-06
Regulation of cell cycle	2.43E-08
Regulation of cholesterol absorption	1.02E-05
EGF receptor signaling pathway	1.59E-09
Ubiquitin cycle	4.71E-05

in CH-B. Despite the activated T cell responses in CH-B, chemokine expression was induced more in the lymphocytes in CH-C than lymphocytes in CH-B (Fig. 4A). To examine the functional role of liver-infiltrating lymphocytes further, LCM samples were also obtained from 4 more patients with CH-B and 4 with CH-C. Gene expression was compared for lymphocyte subsets (84 CD markers, including 26 T cell makers, 21 B cell markers, 16 myeloid cell markers, 11 NK cell markers, and 12 AD markers). Among these, many T cell markers and Th1 cytokines were significantly more upregulated in CH-B than in CH-C lymphocytes. Conversely, B cell marker, Th2 cytokines, and chemokines were preferentially induced in CH-C (Fig. 4B-C). The differences in immune reaction in CH-B and CH-C may be a reflection of their different pathogenesis.

Detailed Gene Network Analysis of Differentially Expressed Genes in CH-B and CH-C. To obtain a detailed and comprehensive gene network underlying CH-B and CH-C, SAGE data were integrated with those from cDNA microarray analysis. We applied 361 upregulated genes in CH-B ($P < .05$) and 344 in CH-C ($P < .05$), obtained from cDNA microarray analysis, and 1924 upregulated genes in CH-B (more than 5-fold tag count differences) and 1780 in CH-C, obtained from SAGE analysis, to the construction of the knowledge-based gene network. To find the gene network among these induced genes, published results of interaction of individual genes were integrated with these results using MetaCore software. Direct interactions between individual genes were searched for. The gene network of these differentially expressed genes formed a complex interaction of individual genes; however, representative signaling pathways underlying CH-B or CH-C were identified (Fig. 5).

In CH-B, p53 and 14-3-3 interacting genes might play an important role in the induced signaling pathways. Transcriptional factors such as CCAAT/enhancer binding protein (C/EBP), c-JUN, and cAMP-responsive element binding protein 1 (CREB1) are possibly also important molecules regulating these signaling pathways. These molecules induced apoptosis and activated transcription and oncogenes. Such activation might activate

Table 6. Gene Ontology Comparison

GO Description	Number of Genes	LS Permutation (P Value)	KS Permutation (P Value)	HBV	HCV	Reference
Whole liver tissue						
Antigen presenting	15	0.00105	0.034	1.01	1.49	0.81
IFN-alpha induced	71	$<1 \times 10^{-5}$	0.000	1.49	2.09	1.16
Cell death	34	0.005	0.019	1.35	1.15	0.99
DNA repair	62	0.005	0.041	1.51	1.10	1.11
G_1/S transition of mitotic cell cycle	18	0.001	0.009	1.25	1.41	1.23
Transcription factor binding	74	0.017	0.001	1.33	1.33	1.30
Cholesterol biosynthesis	12	0.029	0.002	1.11	1.44	1.30
PDGF	22	0.005	0.012	1.08	1.33	1.13
Peroxisome	19	0.026	0.005	1.46	1.17	0.93
Hepatocytes						
Peptidyl-prolyl cis-trans isomerase activity	9	0.002	0.001	1.31	1.48	1.15
Single-stranded DNA binding	16	0.019	0.003	1.85	1.34	1.27
Mitochondria	110	0.005	0.010	0.89	1.52	1.14
IFN-alpha induced	77	0.004	0.146	1.62	5.77	1.35
Lymphocytes						
Immunological synapse	12	0.002	0.003	6.38	3.78	3.31
Induction of apoptosis via deathdomain receptors	7	0.004	0.018	1.53	1.02	1.07
Chemotaxis	54	0.004	0.069	1.35	1.78	1.14

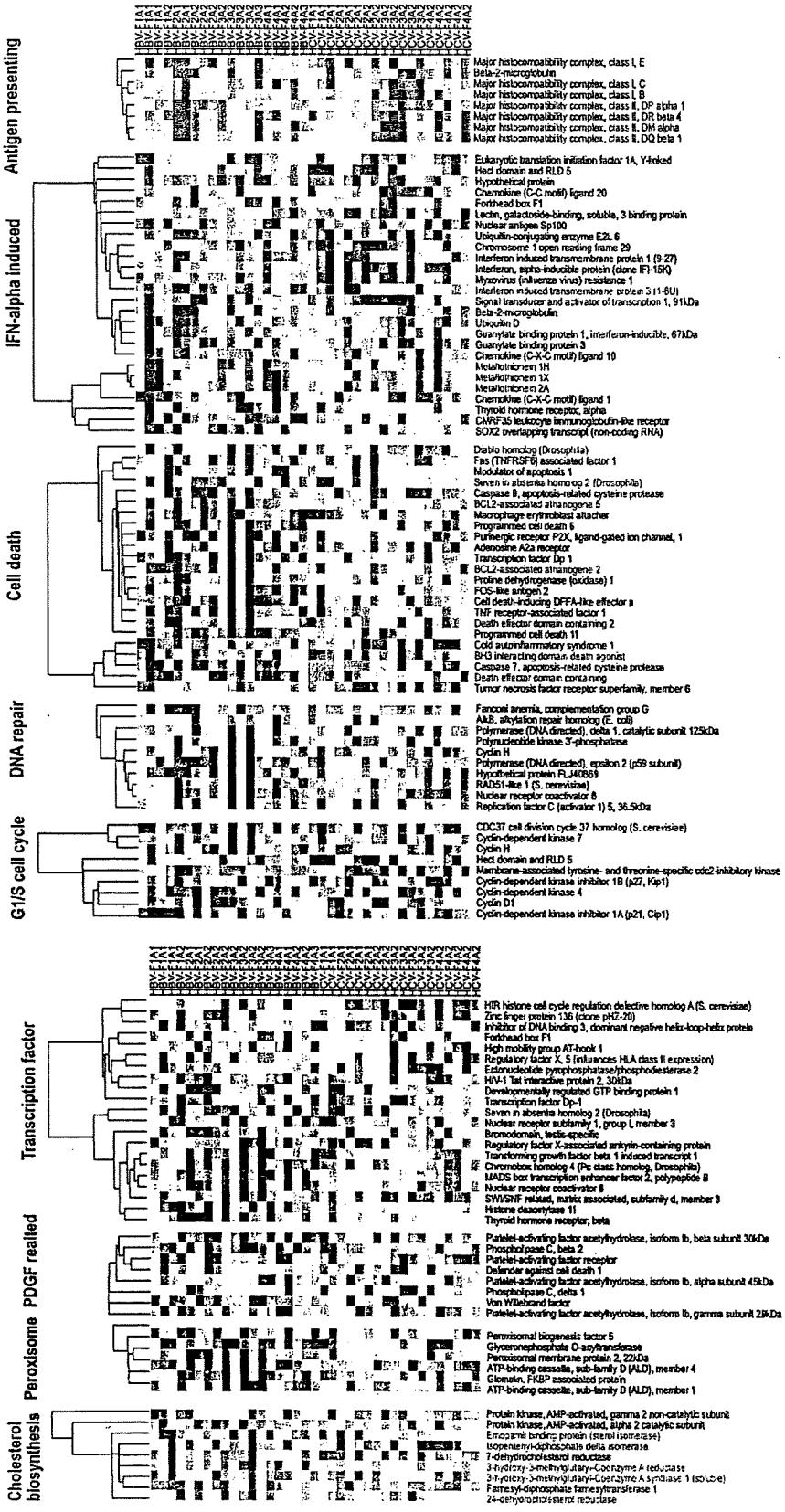

Fig. 3. One-way hierarchical clustering of whole liver samples with representative genes ($P < .05$) included in each GO category which was significantly different in CH-B and CH-C ($P < .005$). Green text denotes genes expressed predominantly in hepatocytes, and blue text denotes genes expressed predominantly in lymphocytes.

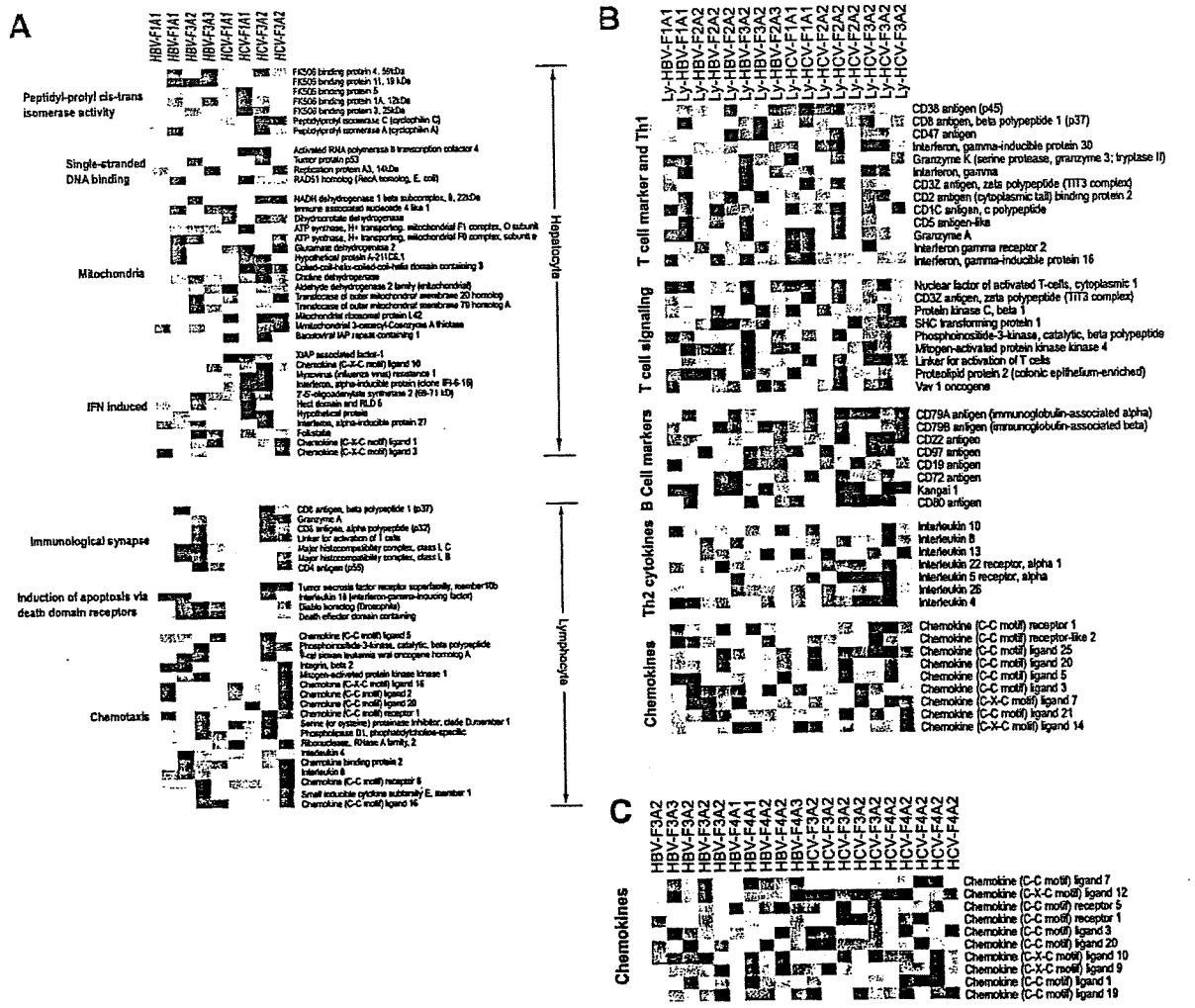

Fig. 4. (A) One-way hierarchical clustering of LCM samples with representative genes ($P < .05$). (B) One-way hierarchical clustering of liver-infiltrating lymphocytes, featuring specific gene sets of immune function. (c) One-way hierarchical clustering of whole liver sample gene sets of chemokines.

peroxisomes in CH-B (Fig. 5). In CH-C, type 1-IFN signaling (ISGF3/STAT1) might play a major role in the induced signaling pathways. The activation of the NF-κB and epidermal growth factor receptor (EGFR) signaling pathways may reflect liver inflammation and regeneration. These activations could lead to activation of liver X receptor/retinoid X receptor (LXR/RXR), a regulator of lipid metabolism.

Based on the database of MetaCore, which covers the entire regulation of the transcriptional factors, transcriptional regulation of differentially expressed genes was analyzed (Table 7). Transcription of mothers against decapentaplegic homolog 3 (SMAD 3), activator protein-1 (AP-1), p53, CREB1, and sterol regulatory element binding transcription factor 1 (SREB-1) was induced in CH-B, whereas NF-κB, IRF-1, STAT1, and retinoid acid receptor-alpha (RARα) signaling pathways were induced in CH-C. These differences fundamentally explain the different signaling pathways in CH-B and CH-C.

To examine whether these differences in gene expression contribute the different mechanism of hepatocarcinogenesis, we compared the angiogenic factors in CH-B and CH-C. The hierarchical clustering of patients using 34 angiogenesis-related genes obtained from cDNA microarray analysis, significantly clustered patients into 2 groups of CH-B or CH-C ($P = .0001$) (Fig. 6A). In CH-B, VEGF-family genes, FGF, and the angiopoietin

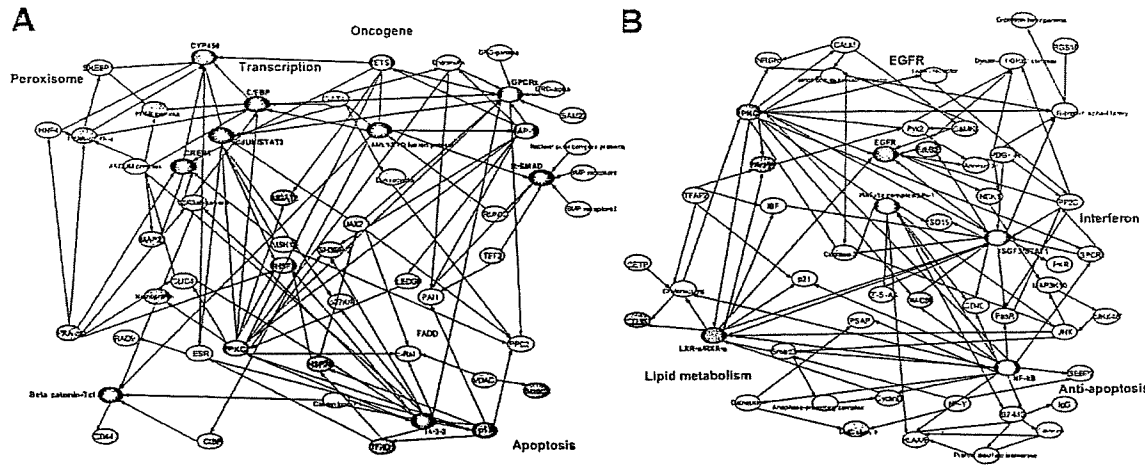

Fig. 5. (A) Gene network of differentially expressed genes in CH-B. (B) Gene network of differentially expressed genes in CH-C. Core transcription factors are represented by black ovals. Green ovals show genes expressed predominantly in hepatocytes and blue ovals show genes expressed predominantly in lymphocytes.

family were induced by several transcriptional factors including AP-1, c-fos, and STAT3, which were all strongly upregulated. In CH-C, inflammation-related angiogenic factors such as IL-8, IL-18, and PDGF1, induced by NF-κB, were also upregulated (Fig. 6B, Fig. 7). Thus, CH-B and CH-C showed different angiogenic properties, which implied that the tumorigenic process in CH-B and CH-C may differ.

Table 7. Transcription Regulation

	Frequent pathway process	*P* value
	Chronic hepatitis B	
1	Mothers against decapentaplegic homolog 3 (SMAD3)	5.25E-36
2	Activator protein-1 (AP-1)	4.24E-33
3	p53	8.49E-33
4	cAMP-responsive element binding protein 1 (CREB1)	2.39E-32
5	v-ets erythroblastosis virus E26 oncogene homolog 1 (ETS1)	3.38E-32
6	Sterol regulatory element binding transcription factor 1 (SREBP1)	6.73E-32
7	Transcription factor binding to IGHM enhancer 3 (TFE3)	9.48E-32
8	Signal transducer and activator of transcription 3 (STAT3)	1.33E-31
9	v-ets erythroblastosis virus E26 oncogene homolog 2 (ETS2)	1.88E-31
10	Transcription factor 7/Lymphoid enhancer binding factor 1 [Tcf(ref)]	1.88E-31
	Chronic hepatitis C	
1	Nuclear factor of κ light polypeptide gene enhancer in B-cells 1 (NF-κB)	1.32E-35
2	Interferon regulatory factor 1 (IRF1)	4.34E-33
3	Splicing factor 1(SF1)	9.17E-33
4	Signal transducer and activator of transcription 1 (STAT1)	1.28E-32
5	Retinoid acid receptor- (RAR)	1.81E-32
6	Nuclear factor of κ light polypeptide gene enhancer in B-cells 2 (RelA)	3.56E-32
7	Vitamin D receptor (VDR)	5.00E-32
8	Wilms tumor 1(WT1)	7.02E-32
9	Sterol regulatory element binding transcription factor 2 (SREBP2)	9.84E-32
10	Epidermal growth factor receptor (EGFR)	1.92E-31

Quantitative RTD-PCR. We performed quantitative real-time detection PCR (RTD-PCR) using 15 TaqMan probes. The results of RTD-PCR on whole liver biopsy and LCM samples are shown in Fig. 7. In CH-B, apoptosis-inducing genes such as CASP9, IFNG, GZMA, TP53, BGA2, and DIABLO were upregulated. In CH-C, IFN-α-induced genes and chemokines such as MxA, IFI15, OAS2, and IP10 were upregulated. Angiogenic factors such as FGFB, ANGPT1, and VEGF were upregulated in CH-B, and another angiogenic factor, PDECGF, was upregulated in CH-C. The results are consistent with those from the cDNA microarray.

Discussion

The biological activity of viral coding polyproteins of HBV and HCV has been extensively investigated in cell lines and in transgenic mouse models. For example, accumulated evidence shows HBV-X protein to be a transcriptional transactivator that interacts with p53 tumor suppressor protein, modulating its signaling pathway.[9,25] The transgenic mouse model with overexpression of HCV polyproteins in the liver develops steatosis and HCC.[26,27] However, these findings have not been well evaluated in clinical samples.

Using in-house cDNA microarray analysis of 1080 genes, we previously reported differing gene expression profiles of liver tissue from patients with CH-B and CH-C.[13] However, the detailed signaling pathways underlying these diseases needed further clarification. In this study,

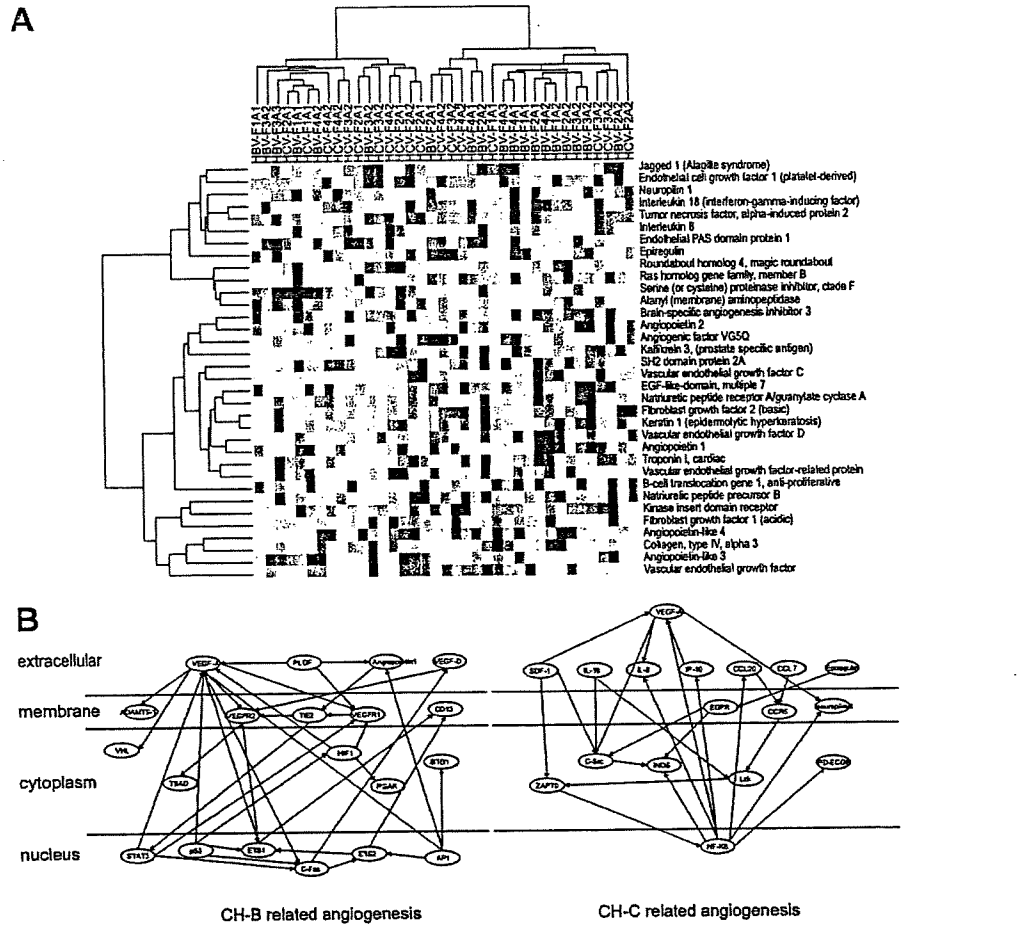

Fig. 6. (A) Hierarchical clustering of whole liver samples using angiogenic genes. (B) Gene network of angiogenic genes in CH-B and CH-C.

we constructed a new microarray slide, liver chip 10 K, consisting of 9614 clones which were selected from unique tag sequences in our hepatic SAGE libraries, including 667,067 tag sequences (manuscript in preparation), for the purpose of analyzing gene expression profiling in liver disease. We analyzed the gene expression profiles of whole liver biopsy specimens obtained from 37 patients with CH-B and CH-C. In addition, we selectively isolated liver-infiltrating lymphocytes (16 samples) and hepatocytes (8 samples) from liver biopsy specimens using LCM (Fig. 1D) and analyzed their gene expression. Furthermore, SAGE data were obtained from pooled samples of 3 CH-B or 3 CH-C patients, and their gene expression data were integrated to reveal the comprehensive, detailed gene network involved in CH-B and CH-C, respectively.

Hierarchical clustering analysis of 37 patients grouped these patients into 2 groups with CH-B or CH-C, with a few exceptions. Moreover, gene prediction analysis significantly discriminated between CH-B and CH-C patients ($P < .001$). HBV or HCV was the only factor significantly involved in patient classification, and other factors such as histological stage, disease activity, age, and ALT levels were not significantly associated with the classification of these patients. This indicates that virus type, whether HBV or HCV, influences liver gene expression to a greater degree than any other clinical parameter, such as degree of fibrosis or inflammation (Table 2).

The pathway analysis and GO comparison in CH-B and CH-C using whole liver biopsy revealed that antigen-presenting genes, IFN-α-induced genes, G_1/S transition genes, and cholesterol biosynthesis and platelet-derived factors were upregulated in CH-C, whereas genes related to cell death, DNA repair, and peroxisomes were upregulated in CH-B (Tables 5-6, Fig. 3). The association of HCV infection with steatosis in the liver in CH-C has

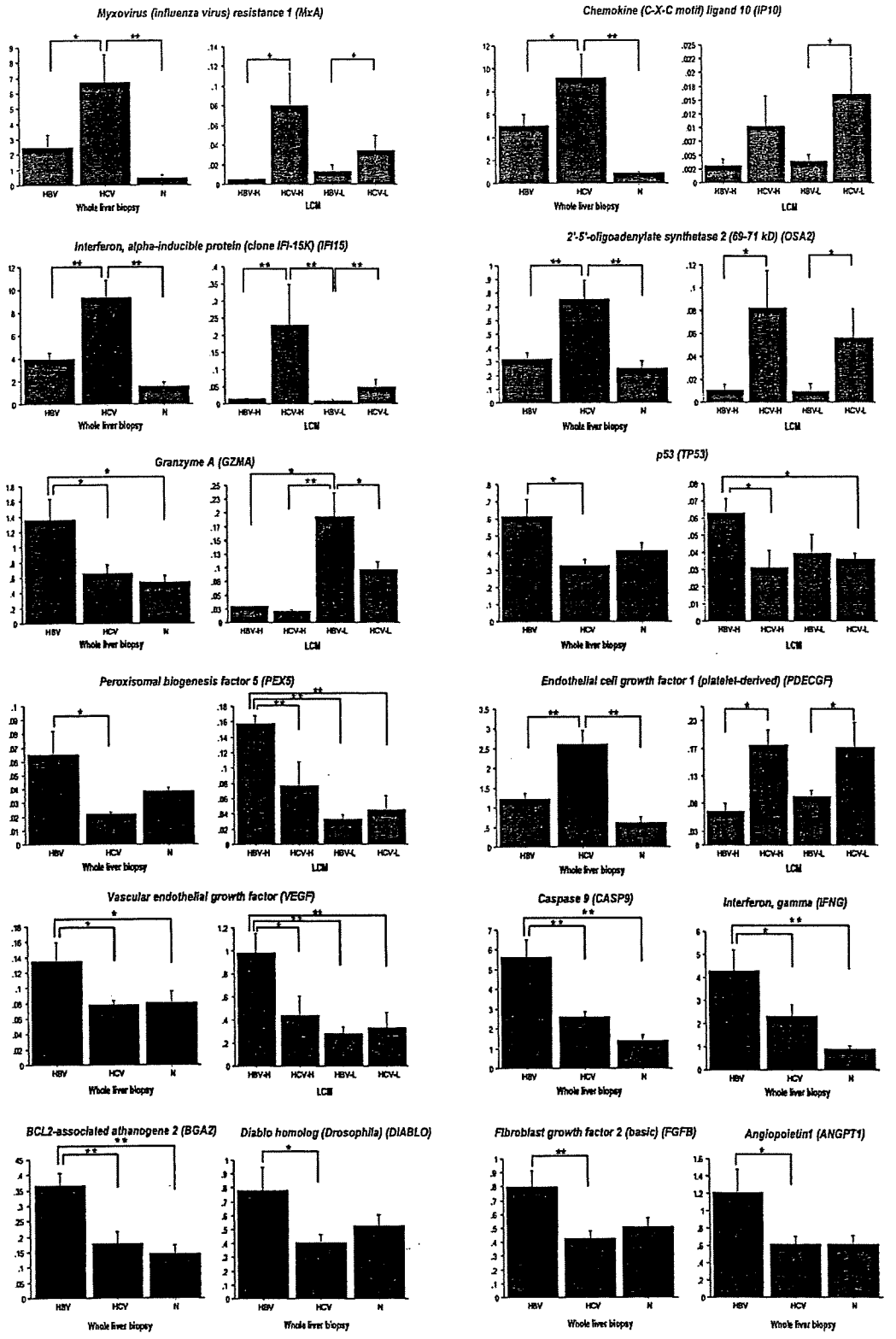

Fig. 7. Quantitative real-time detection PCR (RTD-PCR) using 15 TaqMan probes. The results of whole liver biopsy (HBV; 19 samples of CH-B, HCV; 18 samples of CH-C and N; 6 samples of normal liver) and LCM samples (HBV-H; 4 samples of hepatocyte in CH-B, HCV-H; 4 samples of hepatocyte in CH-C, HBV-Ly; 8 samples of lymphocyte in CH-B, HCV-Ly; 8 samples of lymphocyte in CH-C) were shown. $^{*}P < .05$, $^{**}P < .01$.

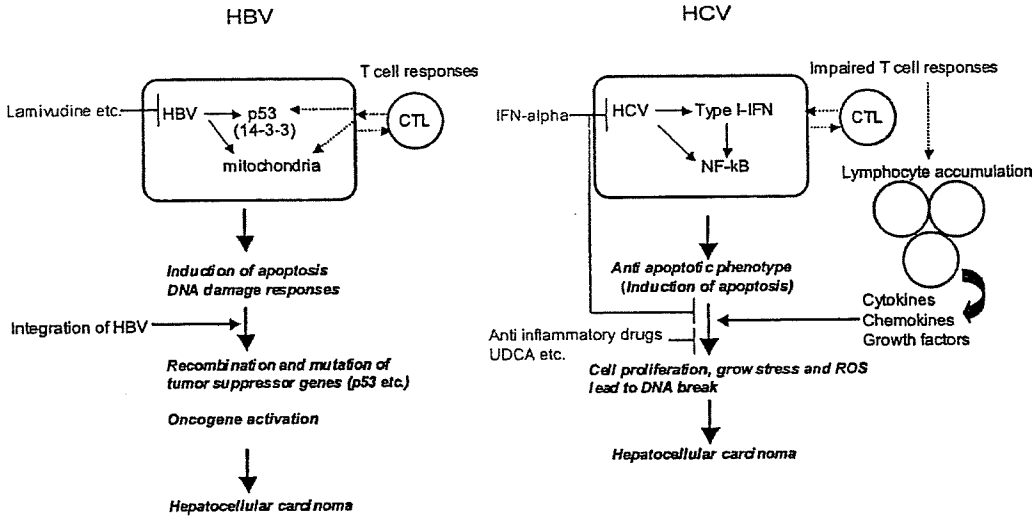

Fig. 8. Schematic representation of different pathogenesis of hepatitis and development of HCC in CH-B and CH-C.

been reported.[28,29] There might also be an association between HBV replication and peroxisomal activation, as reported using hepatoma-derived cell lines.[30,31] We combined SAGE data with those from cDNA microarray analysis and constructed the detailed and comprehensive gene network underlying CH-B and CH-C. In CH-B, p53-mediated and 14-3-3-mediated pro-apoptotic signaling; transcription factors such as AP-1, C/EBP, c-JUN, and CREB1; and oncogenes and peroxisomes were activated (Fig. 5). In CH-C, type 1-IFN (ISGF3/STAT1), NF-κB, EGFR, and LXR/RXR signaling were activated.

Lesion-specific gene expression analysis by LCM revealed more precise differences in gene expression between CH-B and CH-C (Fig. 4, Fig. 7), although a larger number of samples will be needed to reach concrete conclusions. Interestingly, many IFN-α-induced genes were upregulated in hepatocytes, but not in lymphocytes, in CH-C. On the other hand, DNA repair genes such as p53 and RAD were induced in hepatocytes in CH-B. Detailed analysis of lymphocyte markers revealed Th1-dominant responses in the liver in CH-B and Th2-dominant responses in the liver in CH-C.

Despite greater lymphocyte infiltration and homing in the liver, a weak T cell response and no T cell accumulation were observed in CH-C.[32,33] These contributed to the induction of various chemokines, cytokines, and growth factors, which may lead to cell proliferation and angiogenesis in CH-C. Surprisingly, gene expression profiling of angiogenic factors revealed clear differences in CH-B and CH-C. Many of the chemokines involved in angiogenesis are independent of VEGF-mediated or angiopoietin-mediated signaling pathways.[34] These findings possibly reflect a different means of carcinogenesis of HCC in CH-B and CH-C (Fig. 6).

In summary, we investigated the detailed signaling pathways in CH-B and CH-C. Although our data reveal the different signaling pathways induced in CH-B and CH-C, the precise mechanisms underlining these differences must be proven experimentally in the future. Nevertheless, from the therapeutic point of view, these results might be indicative that antiviral agents will be most effective for CH-B whereas anti-inflammatory drugs, other than IFN, would be effective for CH-C, for the prevention of HCC (Fig. 8). Further studies are needed to elucidate these findings clinically and biologically.

Acknowledgment: We thank Masami Ueda and Mikiko Nakamura for excellent technical assistance.

References

1. Shafritz DA, Shouval D, Sherman HI, Hadziyannis SJ, Kew MC. Integration of hepatitis B virus DNA into the genome of liver cells in chronic liver disease and hepatocellular carcinoma. Studies in percutaneous liver biopsies and post-mortem tissue specimens. N Engl J Med 1981;305:1067-1073.
2. Choo QL, Kuo G, Weiner AJ, Overby LR, Bradley DW, Houghton M. Isolation of a cDNA clone derived from a blood-borne non-A, non-B viral hepatitis genome. Science 1989;244:359-362.
3. Kiyosawa K, Sodeyama T, Tanaka E, Gibo Y, Yoshizawa K, Nakano Y, et al. Interrelationship of blood transfusion, non-A, non-B hepatitis and hepatocellular carcinoma: analysis by detection of antibody to hepatitis C virus. HEPATOLOGY 1990;12:671-675.
4. Huang HP, Tsuei DJ, Wang KJ, Chen YL, Ni YH, Jeng YM, et al. Differential integration rates of hepatitis B virus DNA in the liver of children with chronic hepatitis B virus infection and hepatocellular carcinoma. J Gastroenterol Hepatol 2005;20:1206-1214.

5. Minami M, Daimon Y, Mori K, Takashima H, Nakajima T, Itoh Y, et al. Hepatitis B virus-related insertional mutagenesis in chronic hepatitis B patients as an early drastic genetic change leading to hepatocarcinogenesis. Oncogene 2005;24:4340-4348.
6. Kim CM, Koike K, Saito I, Miyamura T, Jay G. HBx gene of hepatitis B virus induces liver cancer in transgenic mice. Nature 1991;351:317-320.
7. Murakami S, Cheong JH, Kaneko S. Human hepatitis virus X gene encodes a regulatory domain that represses transactivation of X protein. J Biol Chem 1994;269:15118-15123.
8. Murakami S, Cheong J, Ohno S, Matsushima K, Kaneko S. Transactivation of human hepatitis B virus X protein, HBx, operates through a mechanism distinct from protein kinase C and okadaic acid activation pathways. Virology 1994;199:243-246.
9. Lin Y, Nomura T, Yamashita T, Dorjsuren D, Tang H, Murakami S. The transactivation and p53-interacting functions of hepatitis B virus X protein are mutually interfering but distinct. Cancer Res 1997;57:5137-5142.
10. Yasui K, Wakita T, Tsukiyama-Kohara K, Funahashi SI, Ichikawa M, Kajita T, et al. The native form and maturation process of hepatitis C virus core protein. J Virol 1998;72:6048-6055.
11. Hsieh TY, Matsumoto M, Chou HC, Schneider R, Hwang SB, Lee AS, et al. Hepatitis C virus core protein interacts with heterogeneous nuclear ribonucleoprotein K. J Biol Chem 1998;273:17651-17659.
12. Colombari R, Dhillon AP, Piazzola E, Tomezzoli AA, Angelini GP, Capra F, et al. Chronic hepatitis in multiple virus infection: histopathological evaluation. Histopathology 1993;22:319-325.
13. Honda M, Kaneko S, Kawai H, Shirota Y, Kobayashi K. Differential gene expression between chronic hepatitis B and C hepatic lesion. Gastroenterology 2001;120:955-966.
14. Desmet VJ, Gerber M, Hoofnagle JH, Manns M, Scheuer PJ. Classification of chronic hepatitis: diagnosis, grading and staging. HEPATOLOGY 1994;19:1513-1520.
15. Shirota Y, Kaneko S, Honda M, Kawai HF, Kobayashi K. Identification of differentially expressed genes in hepatocellular carcinoma with cDNA microarrays. HEPATOLOGY 2001;33:832-840.
16. Kawai HF, Kaneko S, Honda M, Shirota Y, Kobayashi K. Alpha-fetoprotein-producing hepatoma cell lines share common expression profiles of genes in various categories demonstrated by cDNA microarray analysis. HEPATOLOGY 2001;33:676-691.
17. Kawaguchi K, Honda M, Yamashita T, Shirota Y, Kaneko S. Differential gene alteration among hepatoma cell lines demonstrated by cDNA microarray-based comparative genomic hybridization. Biochem Biophys Res Commun 2005;329:370-380.
18. Honda M, Kawai H, Shirota Y, Yamashita T, Kaneko S. Differential gene expression profiles in stage I primary biliary cirrhosis. Am J Gastroenterol 2005;100:2019-2030.
19. Honda M, Kawai H, Shirota Y, Yamashita T, Takamura T, Kaneko S. cDNA microarray analysis of autoimmune hepatitis, primary biliary cirrhosis and consecutive disease manifestation. J Autoimmun 2005;25:133-140.
20. Yamashita T, Hashimoto S, Kaneko S, Nagai S, Toyoda N, Suzuki T, et al. Comprehensive gene expression profile of a normal human liver. Biochem Biophys Res Commun 2000;269:110-116.
21. Yamashita T, Kaneko S, Hashimoto S, Sato T, Nagai S, Toyoda N, et al. Serial analysis of gene expression in chronic hepatitis C and hepatocellular carcinoma. Biochem Biophys Res Commun 2001;282:647-654.
22. Mootha VK, Lindgren CM, Eriksson KF, Subramanian A, Sihag S, Lehar J, et al. PGC-1alpha-responsive genes involved in oxidative phosphorylation are coordinately downregulated in human diabetes. Nat Genet 2003; 34:267-273.
23. Watashi K, Ishii N, Hijikata M, Inoue D, Murata T, Miyanari Y, et al. Cyclophilin B is a functional regulator of hepatitis C virus RNA polymerase. Mol Cell 2005;19:111-122.
24. Nakagawa M, Sakamoto N, Tanabe Y, Koyama T, Itsui Y, Takeda Y, et al. Suppression of hepatitis C virus replication by cyclosporin a is mediated by blockade of cyclophilins. Gastroenterology 2005;129:1031-1041.
25. Lin Y, Nomura T, Cheong J, Dorjsuren D, Iida K, Murakami S. Hepatitis B virus X protein is a transcriptional modulator that communicates with transcription factor IIB and the RNA polymerase II subunit 5. J Biol Chem 1997;272:7132-7139.
26. Moriya K, Fujie H, Shintani Y, Yotsuyanagi H, Tsutsumi T, Ishibashi K, et al. The core protein of hepatitis C virus induces hepatocellular carcinoma in transgenic mice. Nat Med 1998;4:1065-1067.
27. Lerat H, Honda M, Beard MR, Loesch K, Sun J, Yang Y, et al. Steatosis and liver cancer in transgenic mice expressing the structural and nonstructural proteins of hepatitis C virus. Gastroenterology 2002;122:352-365.
28. Adinolfi LE, Gambardella M, Andreana A, Tripodi MF, Utili R, Ruggiero G. Steatosis accelerates the progression of liver damage of chronic hepatitis C patients and correlates with specific HCV genotype and visceral obesity. HEPATOLOGY 2001;33:1358-1364.
29. Monto A, Alonzo J, Watson JJ, Grunfeld C, Wright TL. Steatosis in chronic hepatitis C: relative contributions of obesity, diabetes mellitus, and alcohol. HEPATOLOGY 2002;36:729-736.
30. Raney AK, Kline EF, Tang H, McLachlan A. Transcription and replication of a natural hepatitis B virus nucleocapsid promoter variant is regulated in vivo by peroxisome proliferators. Virology 2001;289:239-251.
31. Guidotti LG, Eggers CM, Raney AK, Chi SY, Peters JM, Gonzalez FJ, et al. In vivo regulation of hepatitis B virus replication by peroxisome proliferators. J Virol 1999;73:10377-10386.
32. Murakami J, Shimizu Y, Kashii Y, Kato T, Minemura M, Okada K, et al. Functional B-cell response in intrahepatic lymphoid follicles in chronic hepatitis C. HEPATOLOGY 1999;30:143-150.
33. Racanelli V, Sansonno D, Piccoli C, D'Amore FP, Tucci FA, Dammacco F. Molecular characterization of B cell clonal expansions in the liver of chronically hepatitis C virus-infected patients. J Immunol 2001;167:21-29.
34. Guleng B, Tateishi K, Ohta M, Kanai F, Jazag A, Ijichi H, et al. Blockade of the stromal cell-derived factor-1/CXCR4 axis attenuates in vivo tumor growth by inhibiting angiogenesis in a vascular endothelial growth factor-independent manner. Cancer Res 2005;65:5864-5871.

Available online at www.sciencedirect.com
ScienceDirect
Hepatology Research 36 (2006) 167–175
HEPATOLOGY RESEARCH
http://www.elsevier.com/locate/hepres

Virological effects and safety of combined double filtration plasmapheresis (DFPP) and interferon therapy in patients with chronic hepatitis C: A preliminary study

Tatsuya Yamashita*, Kuniaki Arai, Akito Sakai, Eishiro Mizukoshi, Yoshio Sakai, Takashi Kagaya, Yasunari Nakamoto, Masao Honda, Takashi Wada, Hitoshi Yokoyama, Shuichi Kaneko

Department of Gastroenterology and Nephrology, Kanazawa University Graduate School of Medical Science, 13-1 Takara-Machi, Kanazawa, Ishikawa, Japan

Received 3 March 2006; received in revised form 11 July 2006; accepted 22 July 2006
Available online 7 September 2006

Abstract

Purpose: In patients with chronic genotype 1b hepatitis C and a high viral load, the viral load was reduced by double filtration plasmapheresis (DFPP), followed by combined interferon and ribavirin therapy. The safety and virological effects of this treatment method were preliminarily investigated.
Methods: In nine patients with chronic hepatitis C, DFPP was performed three times on days 1, 2, and 4, and the administration of interferon and ribavirin was initiated immediately after DFPP on day 1.
Result: The HCV RNA was undetectable in all patients after the plasma was passed through a plasma fractionator (second filter) in the DFPP circuit. After 2 weeks, the HCV RNA tended to decrease in the DFPP group more than in the control group (-2.45 ± 1.12 versus -1.57 ± 0.95, $P = 0.073$). However, this decrease was not attributable to a sustained virological response (SVR) (22.2% versus 18.2%, $P = 0.822$). Most of the adverse events were caused by the interferon and ribavirin combination therapy.
Conclusion: DFPP can be safely performed concomitantly with interferon and ribavirin combination therapy in chronic hepatitis C patients. The combination may contribute to an early virological response. The effect of DFPP on the SVR and its significance remain to be clarified.

Keywords: Chronic hepatitis C; Interferon therapy; Double filtration plasmapheresis

1. Introduction

Hepatitis C virus (HCV) infection induces acute hepatitis, and approximately 70–80% of these cases progress to chronic hepatitis. The course of the disease is stable in approximately 30% of chronic hepatitis cases; however, the remaining 70% of cases progress to liver cirrhosis after approximately 30–40 years. Further, the cases that progress to liver cirrhosis develop hepatocellular carcinoma at an annual rate of approximately 8% [1].

From the viewpoint of viral eradication, interferon therapy is the only radical therapy for chronic hepatitis C. Once complete viral elimination is achieved by interferon therapy, liver fibrosis improves, and the risk of liver carcinogenesis is reduced [1].

In interferon therapy for chronic hepatitis C, administration of $(3–6) \times 10^6$ IU interferon alone, three times a week for 24 and 48 weeks, has been reported to produce a sustained virological response (SVR) in approximately 6% and 16% of patients, respectively [2]. Treatment with interferon in combination with ribavirin for 24 and 48 weeks has been reported to produce an SVR in 21% [3] and 41% [2,4,5] of patients, respectively.

* Corresponding author. Tel.: +81 76 265 2235; fax: +81 76 234 4250.
E-mail address: ytatsuya@m-kanazawa.jp (T. Yamashita).

1386-6346/$ – see front matter
doi:10.1016/j.hepres.2006.07.013

A combination of pegylated interferon (PEG-IFN) – a recently marketed long-acting interferon for once-a-week administration – and ribavirin induced an SVR in 47% of patients with chronic genotype 1b HCV infection and high viral loads in whom previous interferon therapy failed to produce a response [6,7].

However, even the combination therapy with PEG-IFN and ribavirin for 48 weeks, which is currently the most promising therapy, does not improve viremia in the other patients for whom there is no appropriate therapy for the eradication of HCV viremia other than time-course observation and the administration of liver-protective drugs. An NS3 protease inhibitor has been developed as a novel antiviral agent, and clinical studies have been performed using this agent; however, the clinical application of this drug will take time because of the occurrence of certain adverse events [8]. The development of an NS5 polymerase inhibitor and an internal ribosome entry site (IRES)-targeting agent is in progress [9–11].

The presence or absence of concomitant ribavirin therapy, the duration of therapy, the virus genotype, the viral load before administration, the grade of liver fibrosis, and the gender and age of the patient are all factors that influence the therapeutic effect of interferon therapy. An early virological response (EVR) is defined as a decline of more than 2 $\log_{10}$ units in the viral load 8 or 12 weeks after the initiation of treatment; it has also been reported to be one of the important factors for an SVR [12,13].

There have been several studies in which the HCV level was investigated in HCV-positive patients during extracorporeal circulation therapies, such as plasmapheresis and hemodialysis. In these studies, the HCV RNA level decreased transiently by approximately 50–90% immediately after plasmapheresis or hemodialysis; however, it returned to either the pre-treatment level or to a higher level within approximately 4–6 h [14–17].

In double filtration plasmapheresis (DFPP), which is a plasmapheresis therapy, the patient's whole blood is separated into plasma and blood cell components by using a plasma separator (first filter). The separated plasma components are further separated into high and low molecular weight components by using a plasma fractionator (second filter); the high molecular weight components including immunoglobulins are removed, and the low molecular weight components including albumin are returned to the body. Although this technique using two filters is relatively more complicated than the normal simple plasma exchange, its advantage is that supplemental plasma transfusion is not necessary.

The diameter of the HCV particle is approximately 55–65 nm [18]. In theory, these viruses are unable to pass through the second filter that has a pore size smaller than the diameter of the viral particle; they are therefore eliminated from the plasma.

In this study, we attempted to reduce the viral loads of patients with chronic genotype 1b hepatitis C and a high viral load by using DFPP. We focused on HCV RNA levels both before plasmapheresis therapy and before interferon and ribavirin combination therapy, and then investigated the early virological effects and also the safety of the treatment.

2. Experimental/materials and methods

2.1. Patients

The study involved nine patients (four males and five females, mean age: 51.7 ± 11.3 years) with chronic genotype 1b hepatitis C that was histologically diagnosed at our department between December 2002 and July 2004. In these patients, the HCV RNA level determined by reverse transcriptase-polymerase chain reaction (RT-PCR) was not less than 100 KIU/ml.

The inclusion criteria were as follows. (1) Minimum age: 20 years; maximum age: 70 years. (2) Blood test values before therapy: hemoglobin, 12 g/dl or higher; platelet count, 100,000 mm^{-3} or higher; white blood cell count, 3000 mm^{-3} or higher; neutrophil count, 1500 mm^{-3} or higher.

The exclusion criteria were as follows. (1) Pregnancy or possible pregnancy, and lactation; (2) depression; (3) serious complications, particularly uncontrollable hypertension and impaired function of the bone marrow, kidneys, or the lungs; (4) autoimmune diseases or suspicion of the same; (5) diabetes or suspicion of the same; (6) allergic predispositions; (7) history of hypersensitivity to interferon or nucleic acid analogues; (8) history of hypersensitivity to biological products such as vaccines; (9) suspicion of alcoholic liver injury, autoimmune hepatitis, or drug-induced liver injury; (10) multiple infections with hepatitis B virus within 48 weeks before the initiation of therapy or suspicion of the same; (11) previous hepatic encephalopathy, rupture of the esophageal varix, orascites; (12) complications of hepatic cirrhosis or hepatocellular carcinoma on examination within 4 weeks before the initiation of therapy or ongoing treatment for the same; (13) treatment with drugs having antiviral actions, immunoregulatory actions, or bone marrow-inhibiting actions such as interferon, Ara-A, zidopudine, glucocorticoid, interleukin 2, or Shosaikoto within 12 weeks of the initiation of therapy or administration of injections containing glycyrrhizin as the main ingredient, theophylline, antipyrine, or warfarin within 4 weeks before therapy.

2.2. Study design

This study was conducted in accordance with the Good Clinical Practice guidelines, conforming to the Helsinki Declaration. It was approved by the Ethics Committee of Kanazawa University Clinical Study Center, and written informed consent was obtained from the patients before their participation in the study.

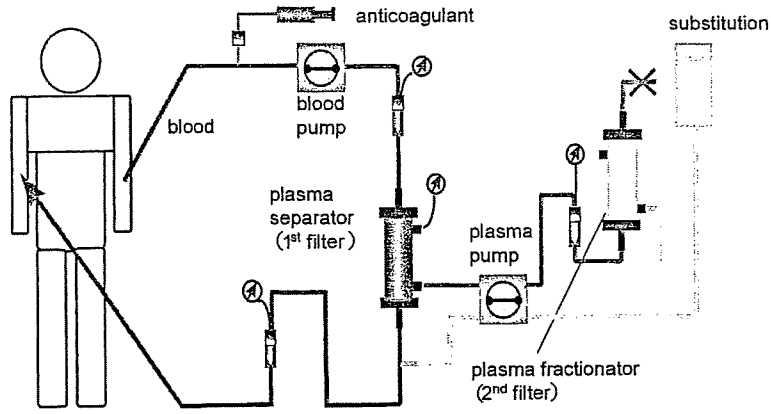

Fig. 1. Mechanism of double filtration plasmapheresis (DFPP). The blood is separated into plasma and blood corpuscles by the plasma separator (first filter), and then filtered using a plasma fractionator (second filter) which separates the plasma into low- and high-molecular weight components.

2.2.1. Treatment schedule

DFPP was performed on day 1 of the therapy to decrease the viral load, and the administration of interferon and ribavirin was initiated 1 h after the completion of DFPP. DFPP was performed three times, on days 1, 2, and 4, and a blood test was performed before each treatment to determine the efficacy of the treatment.

2.2.2. Double filtration plasmapheresis

In order to access the blood during DFPP, a Soft-Cell double-lumen catheter (GamCath catheter N®; Gambro, Stockholm, Sweden) was inserted and indwelled in the right femoral vein for 5 days.

For DFPP, a Plasmaflo KM8800 (Kuraray Medical Inc., Tokyo, Japan) was used as the dialysis apparatus. The plasma separator and plasma fractionator (first and second filters, respectively) used were Plasmaflo OP-08W® and Cascadeflo EC-50W®, respectively (Asahi Kasei Medical Co. Ltd., Tokyo, Japan) (Fig. 1). With regard to the frequency of treatment, in a previous study it was observed that the level of fibrinogen decreased to less than 100 mg/dl when DFPP was continuously performed twice. Thus, DFPP was discontinued on day 3 to prevent fibrinogen-associated complications, such as a tendency to bleed, and the applicability of DFPP on day 4 was determined based on laboratory test results.

In order to process 50 ml/kg of blood in a single round of DFPP, DFPP was performed for approximately 3 h at a blood flow rate of approximately 80 ml/min. The potent protease inhibitor, Nafamostat mesilate (Naotamin®; Asahi Kasei Pharma Co. Ltd., Tokyo, Japan), was used as an anticoagulant because heparin is considered to influence RT-PCR when this procedure is used for HCV RNA measurement. For fluid replacement, we used either 50 or 100 ml of 25% albumin (Kenketsu Albumin-Wf®; Mitsubishi Pharma Co., Tokyo, Japan) that was diluted with 200 ml of saline.

Blood tests were performed before each DFPP to ensure that the plasmapheresis could be performed without the occurrence of any adverse events; DFPP was not performed if the platelet count was 50,000 mm^{-3} or less, or if the fibrinogen level was 100 mg/dl or less. The DFPP was resumed after the recovery of these test values was confirmed.

2.2.3. Interferon therapy

For the interferon therapy, interferon (IFN) α-2b (Intron A®; Schering-Plough KK, Kenilworth, NJ) and ribavirin (Rebetol®; Schering-Plough KK) were concomitantly administered. IFN α-2b was administered intramuscularly 1 h after the completion of DFPP on day 1; the oral administration of ribavirin was initiated after the completion of DFPP on day 1. IFN α-2b was administered six times a week for 2 weeks at a daily dose of 6×10^6 IU, followed by three times a week for 22 weeks or three times a week intermittently for 46 weeks. The ribavirin dose was determined based on the body weight measured at the time of patient registration. The dose used was 600 and 800 mg for body weights of less than 60 and 60 kg or higher, respectively. The daily dose was divided into two doses and administered orally for 24 weeks.

2.2.4. Evaluation

The HCV RNA was measured during and after therapy by using an RT-PCR assay (Amplicor HCV RNA Monitor®; BML, Tokyo, Japan: measurement sensitivity, 0.5 KIU or higher); the sample was diluted when the HCV RNA level was higher than the upper quantification limit (850 KIU/ml). When the HCV RNA was less than the lower quantification limit, a qualitative method was used (Amplicor HCV RNA®, BML; measurement sensitivity, 50 IU).

The HCV RNA was measured after 2, 4, 8, and 12 weeks of therapy, either before DFPP or every morning on days 1–6. It was measured after 24 and 48 weeks of therapy as well as at 24 weeks after the completion of the interferon therapy. Whenever possible, the HCV RNA was also measured immediately after DFPP completion. The HCV RNA in the plasma before and after the second filtration in the DFPP circulation was also measured 1 h after the initiation of the DFPP and immediately before the completion of the DFPP. A negative

viral detection at 24 weeks after the interferon administration was defined as an SVR.

As a control group for a comparison of the decrease in HCV RNA during the 2-week therapy period, we used the HCV RNA data of 11 patients with chronic genotype 1b hepatitis C and a high viral load who underwent IFN and ribavirin combination therapy without DFPP at our department during the same period.

In all patients, a liver biopsy was performed immediately before therapy, and fibrosis and inflammation were evaluated based on the New Inuyama classification. The inflammatory activity in the portal vein and the periportal area as well as the degrees of intralobular inflammation and hepatocyte degeneration were graded from A0 to A3 (0: none, 1: mild, 2: moderate, and 3: severe) based on the "degree of inflammatory activity". Fibrosis was also graded from F0 to F4 (0: none, 1: mild without septa, 2: moderate with few septa, 3: numerous septa without cirrhosis, and 4: cirrhosis) [19].

For the blood tests, we performed white blood cell, red blood cell, platelet, and differential leukocyte (neutrophils, eosinophils, basophils, lymphocytes, and monocytes) counts as well as the zinc sulfate turbidity test (ZTT). Further, the percentage of hemoglobin, hematocrit, and reticulocytes as well as the levels of fibrinogen, total protein, albumin, γ-globulin, and total cholesterol were all measured.

Adverse events were evaluated in accordance with the WHO guidelines, and these were classified into mild, moderate, severe, and life-threatening events.

The significance of the differences was analyzed using the χ^2-test, Fisher's exact test, a *t*-test, and logistic regression analysis.

3. Results

3.1. Patients' backgrounds

The patients' backgrounds are listed in Table 1. In the DFPP group, there were four male and five female patients with a mean age of 51.7 ± 11.3 years. The HCV RNA before therapy was at least 100 KIU/ml and less than 500 KIU/ml in three patients and 500 KIU/ml or higher in six patients, indicating that many of the patients had a high viral load. Three patients had previously undergone IFN therapy, which was virologically ineffective. For the remaining six patients, this was their first experience of IFN therapy. With regard to liver histology, the fibrosis was graded as F2 or lower in all patients, and in all patients there was no evidence of advanced chronic hepatitis. Compared with the control group, gender, age, serum HCV RNA, previous IFN treatment, liver histology, and blood biochemical data for the treatment group were statistically not significantly different.

3.2. Virological changes after DFPP

To confirm the elimination of the virus by DFPP, HCV RNA was measured before and after the second filtration. One hour after the initiation of DFPP, once the DFPP exchange blood flow had stabilized, the HCV RNA in the blood after it had passed through the second filter was quantitatively undetectable in all nine patients. This confirmed the elimination of the virus by the second filter (Fig. 2). Further, at the completion of DFPP – approximately 3 h after its initiation – the HCV RNA was undetectable in all nine patients (data not shown). These findings confirmed that DFPP is capable of

Table 1
Baseline characteristics of chronic genotype 1b hepatitis C patients with a high viral load, treated with a combination of DFPP with interferon (IFN) and ribavirin therapy (DFPP group) and IFN and ribavirin therapy without DFPP (control group)

	DFPP + IFN-R	IFN-R	*P*-value
Gender (M/F)	4/5	7/4	0.684
Age	51.7 ± 11.3	50.6 ± 10.6	0.856
Serum HCV RNA (KIU/ml)			
Mean (minimum–maximum)	2162 (224–12000)	818 (340–1700)	0.254
100–500/500≦	3/6	3/8	
Previous IFN treatment			
Naïve/retreatment	6/3	5/6	0.343
Liver histology			
Stage (F0/F1/F2/F3/F4)	1/1/7/0/0	0/5/6/0/0	0.167
Grade (A0/A1/A2/A3)	0/5/3/1	1/7/3/0	0.541
ALT (IU/ml)	88.4 ± 47.7	89.5 ± 34.5	0.957
Hemoglobin (g/dl)	14.0 ± 1.7	14.2 ± 1.2	0.728
Platelet count ($\times 10^4$ μl^{-1})	16.9 ± 5.2	15.7 ± 3.4	0.551
Fibrinogen (mg/dl)	231.0 ± 38.9	222.7 ± 92.3	0.804
ZTT (IU)	12.4 ± 4.9	14.2 ± 6.4	0.496
Total protein (mg/dl)	6.9 ± 0.4	6.9 ± 0.4	>0.999
Albumin (g/dl)	4.2 ± 0.3	4.1 ± 0.4	0.373
γ-Globulin (g/dl)	1.3 ± 0.2	1.4 ± 0.3	0.492
Total cholesterol (mg/dl)	178.6 ± 28.3	172.0 ± 45.2	0.714

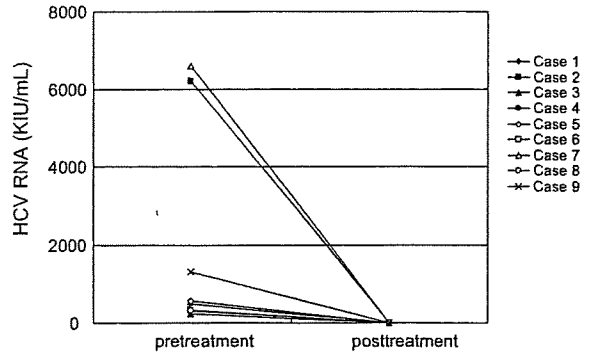

Fig. 2. Change in plasma HCV RNA pre- and post-plasma fractionator (second filter). In all nine cases, HCV RNA was not detected in the plasma of the post-plasma fractionator filtrate 1 h after starting the DFPP.

eliminating the HCV particles and that the elimination efficiency does not decrease with time.

3.3. Early virological response

In order to investigate the EVR, the HCV RNA was measured 2 weeks after the initiation of therapy. It was quantitatively undetectable in four of the nine patients (44.4%). In the control group treated with IFN and ribavirin combination therapy without DFPP, the HCV RNA was quantitatively undetectable in two patients (18.2%). The number of patients with undetectable HCV RNA 2 weeks after the initiation of therapy was higher in the DFPP group, but the difference was not significant ($P = 0.201$).

The EVR is defined as a viral load decline of 2 $\log_{10}$ units or more from the baseline level at an early stage in the therapy, i.e., 2 weeks after the initiation of the therapy in the case of this study. An EVR was achieved in 6 of the 9 patients in the DFPP group (66.7%) and in 4 of the 11 patients in the control group (36.4%), indicating that the HCV RNA tended to decrease earlier during concomitant DFPP and interferon therapy; however, the difference was not statistically significant ($P = 0.178$, Fig. 3A).

The change in HCV viral load also tended to decline more in the DFPP group than in the control group (-2.45 ± 1.12 versus -1.57 ± 0.95; $P = 0.073$, Fig. 3B).

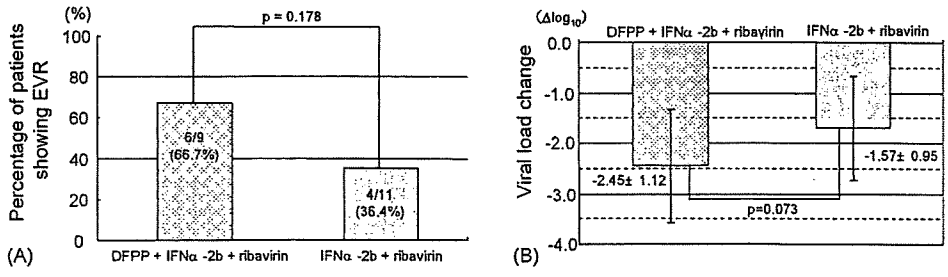

Fig. 3. Change of HCV RNA load 2 weeks after treatment. (A) An EVR is defined as a viral load decline of 2 $\log_{10}$ units or more from the baseline level after 2 weeks of treatment. The numbers in each column indicate the ratio of EVR cases/all treatment cases. (B) Viral load change after 2 weeks. Viral load change was calculated by the formula; $\log_{10}$ (HCV RNA load after 2 weeks/HCV RNA load at pre-treatment).

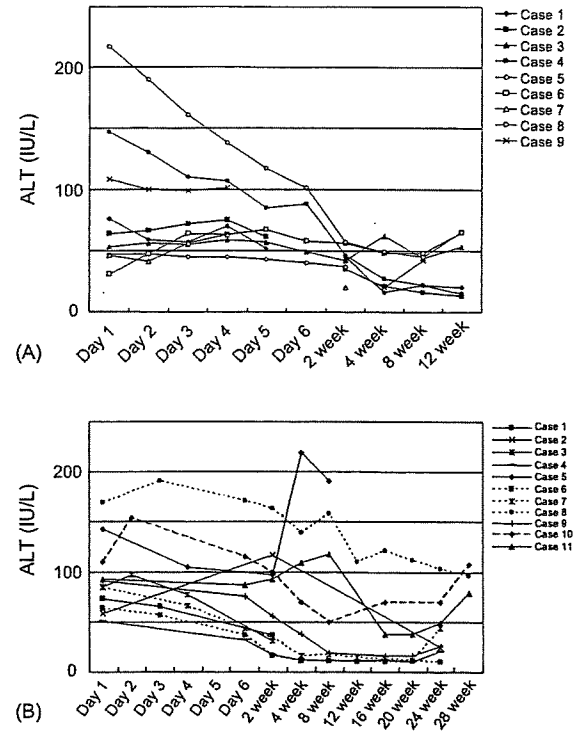

Fig. 4. Change in the serum ALT level during treatment. The ALT level was normalized in eight cases in the second week of treatment.

3.4. Biochemical response

The time-course changes in alanine aminotransferase (ALT) are shown in Fig. 4. The ALT level was normalized in seven of the nine patients (77.8%) by 4 weeks of the therapy. In the control group, it was normalized in 7 of the 11 patients (63.6%). The difference was not statistically significant ($P = 0.845$).

3.5. Sustained virological response

An SVR was observed in two of the nine patients (22.2%) treated with concomitant DFPP and interferon therapy (an intent-to-treat approach). Of these, one patient received IFN

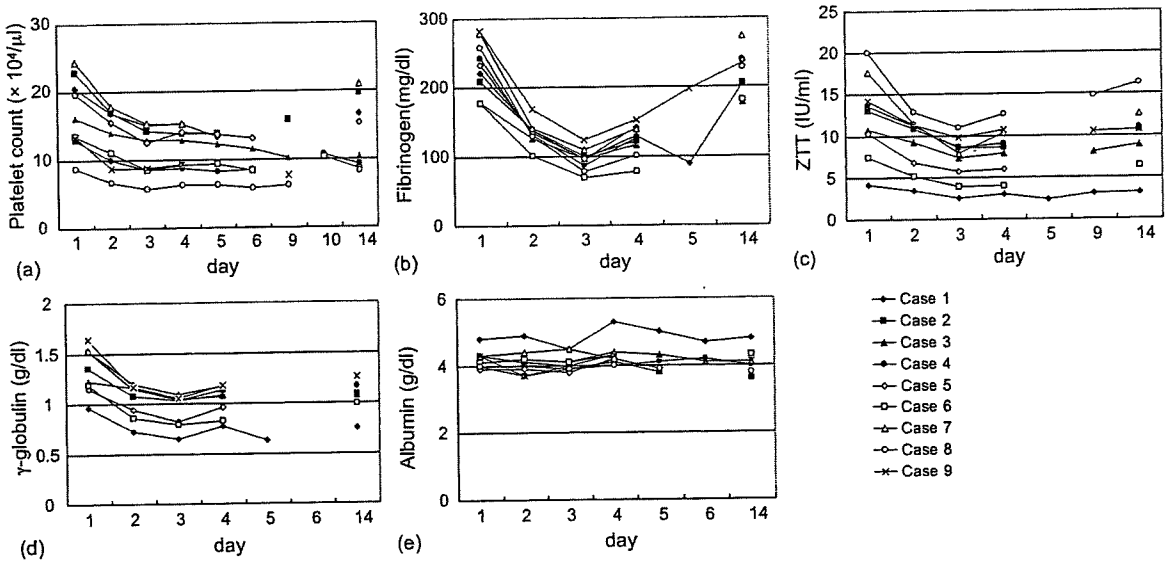

Fig. 5. Changes in the laboratory findings during treatment: (a) platelet count, (b) fibrinogen, (c) ZTT, (d) γ-globulin, and (e) albumin.

and ribavirin combination therapy for 24 weeks, and the other received IFN and ribavirin combination therapy for 24 weeks, followed by additional IFN monotherapy for 24 weeks. These patients were two of the four patients in whom the HCV RNA was quantitatively undetectable after 2 weeks of therapy. Treatment of the other two patients was discontinued before 24 weeks due to adverse events (skin eruption, anorexia, and general malaise). In the six patients for whom complete treatment was possible, the SVR rate was 33.3% (2/6) (a per-protocol approach).

In the control group, the SVR rate was 18. About 2% (2/11) as determined using an intent-to-treat approach and 20.0% (2/10) as determined using a per-protocol approach. The difference in the SVR rate between the two groups was not statistically significant ($P = 0.822$ and 0.551, respectively).

The factors associated with the SVR in our patients were analyzed using uni- and multi-variate analysis. Using univariate analysis, the EVR was found to be the only factor associated with SVR ($P = 0.025$). Associations with other factors, such as DFPP, age, sex, pre-treatment history, and fibrosis, were not detected in our series ($P = 0.822$, 0.170, 0.822, 0.822, and 0.052, respectively). Using multivariate analysis, the association of all of these factors was found to be statistically insignificant.

In the DFPP group, the only factor showing a relationship with the SVR was the viral negativity at 2 weeks ($P = 0.014$).

3.6. Safety and adverse events

In eight of the patients, DFPP was performed three times on days 1, 2, and 4. It was not performed on day 4 in one patient because this patient's fibrinogen level was lower than 100 mg/dl before DFPP; hence, DFPP was performed only twice in this patient.

The changes in laboratory test values as a result of DFPP treatment were also investigated. After DFPP on day 1, the platelet count decreased on average by 22.5%. The decrease persisted until the completion of DFPP and then slowly recovered by 2 weeks after the initiation of the therapy. The fibrinogen level decreased by 30–50% after DFPP on day 1. It decreased to its lowest level on day 3, slowly recovered after the completion of DFPP, and then returned to a level similar to the pre-DFPP level by 2 weeks after the initiation of the therapy. The ZTT values and the γ-globulin and total cholesterol levels also showed similar changes. No change was observed in the serum albumin level (Fig. 5).

The adverse events that occurred during the IFN and DFPP combination therapy are listed in Table 2. Most of these were influenza-like symptoms and digestive symptoms that were associated with the IFN and ribavirin combination therapy. The adverse events attributable to concomitant DFPP and IFN therapy were mild hypotension in two patients and mild

Table 2
Rates of discontinuation of treatment, dose reduction, and occurrence of adverse events during treatment

Adverse events	*n* (%)
Influenza-like symptoms	8 (89)
Skin eruption	1 (11)
Gastrointestinal symptoms	6 (67)
Insomnia	2 (22)
Hypotension	2 (22)
Vagal reflux	1 (11)
Depression	5 (56)
Anemia	7 (78)
Neutropenia	1 (11)
Thrombocytopenia	1 (11)
Dose reduction	4 (44)
Discontinuation of treatment	3 (33)